method used in the present work.

Literature Cited

(1) Castañeda, J. M. B.Sc. Thesis, Fac. de Química, UNAM, México, 1978.
(2) Lozano, F. J.; Garfias, F. J. *Rev. Soc. Quím. Méx.* **1978**, *22*, 436.
(3) Zepeda, J. L.; Lozano, F. J.; Garfias, F. J. *J. Chem. Eng. Data* **1979**, *24*, 287.

Received for review April 24, 1980. Accepted November 4, 1980.

Partial Miscibility Behavior of the Methane–Ethane–*n*-Octane System

J. D. Hottovy, James P. Kohn,* and Kraemer D. Luks

Department of Chemical Engineering, University of Notre Dame, Notre Dame, Indiana 46556

The phase behavior of the ternary system methane–ethane–*n*-octane was studied in the region of immiscibility. Two liquid phases and a vapor phase (L_1–L_2–V) were found to exist in this system in a region extending from 197.8 K and 43.3 atm to ~222 K and 69 atm. Pressure and liquid-phase composition and liquid-phase molar volume data for both of the coexisting liquid phases were measured and are presented as a function of temperature. The immiscibility area was found to be bounded by loci of K points (L_1–L_2 = V), Q points (S–L_1–L_2–V), and LCST points (L_1 = L_2–V).

This study of the methane–ethane–*n*-octane system was undertaken to investigate liquid–liquid–vapor (L–L–V) phenomena that can occur in liquified natural gas (LNG) and natural gas liquid systems. This information is expected to serve as fundamental data with which to evaluate correlations purporting to describe L–L–V behavior in the design of LNG systems.

There are a limited number of binary liquid–liquid–vapor phase equilibria data available for systems rich in methane and ethane relevant to LNG systems. A L–L–V locus has been observed in the system methane–hexane (*1*) and methane–toluene (*2*). Each of these loci terminates at both ends with critical points (L–L = V and L = L–V). A L–L–V locus is observed in the system methane–*n*-heptane (*3*) terminated by a L–L = V critical point and a Q (S–L–L–V) point. Solutes beginning with *n*-octane and higher form crystals before they can become immiscible with methane (*4*).

With ethane as the solvent, solutes beginning with *n*-C_{19} and higher demonstrate L–L–V behavior (*5–7*). With propane, only very long-chain hydrocarbons (*n*-C_{37} and higher) will demonstrate L–L–V behavior (*8*).

Very few L–L–V data exist for ternary or more complex systems relevant to LNG systems. A few observations of L–L–V behavior were made during S–L–V studies (*9, 10*), but many data were taken.

Experimental Section

Materials and Analyses. The methane used in this study was Linde "Ultra Pure" grade stated to be 99.97 mol % pure. The ethane was a Matheson CP grade gas stated to be 99 mol % pure. The methane was used without further purification. However, the ethane was prepared for use by flashing it from the cylinder at room temperature to a 3000-mL storage reservoir maintained at 273.16 K. The vapor phase was then vented from the reservoir to remove the impurities remaining in the vapor phase after liquefaction from the cylinder. The ethane was further purified through activated carbon before use.

Dew-point bubble-point experiments were carried out for both pure gases. For example at 185.06 K, methane exhibited a difference between dew-point and bubble-point pressures of less than 0.20 atm. The ethane had dew-point and bubble-point pressures which differed by 0.24 atm at 273.16 K. The vapor pressures at 50 vol % liquid agreed well with recent literature values for both gases, and the critical temperature and pressure of the ethane was within 0.2 K and 0.1 atm of those given by the National Bureau of Standards (*11*).

The *n*-octane was purchased from the Humphrey-Wilkinson Chemical Co. It had a stated purity of 99 mol %. The measured air-saturated freezing point agreed to within 0.2 K of current literature values. The *n*-octane was used without further purification.

Apparatus and Procedure. The apparatus used in this study was the same as that used by Kohn and others in cryoscopic studies (*9, 12, 13*). Briefly, the procedure involved charging and carefully weighing an amount of *n*-octane in a 10-mL glass cell. This glass cell had previously been calibrated for visual volumetric readings. The cell was then placed in a thermostated liquid bath and chilled until the octane froze. The air in the cell was then removed with a vacuum pump. Separately, ethane and then methane were added to the cell from reservoirs maintained at a convenient pressure by a manually operated syringe-type pump. The *n*-octane was melted by the solvents while being mixed in the cell with a steel ball actuated by an external magnet. The use of separate addition systems for methane and ethane gave improved experimental flexibility.

To obtain a Q point (S–L_1–L_2–V), we lowered the temperature until crystals formed and then raised it until only a trace of crystals remained. It was possible to detect visually as little as a few tenths of a milligram of solid octane in the cell. This was regarded as an equilibrium crystal point (Q point) if two liquid phases were present. By judiciously selecting the amounts of *n*-octane, ethane, and methane added to the cell, we made one of the liquid phases occupy at least 60% (usually more than 80%) of the cell volume. The concentration of ethane in the vapor phase was estimated with the aid of existing literature on methane–ethane vapor–liquid equilibria (*14*). An insignificant amount of octane was assumed to be in the vapor space.

Type-K data points (L_1–L_2 = V) were obtained by increasing the temperature until a sizable L_2 phase (the *n*-octane lean phase) went critical with the vapor phase. This was accompanied with the usual opalescence as the L_2 phase became identical with the vapor phase. For data points where the solute

Table I. Raw Data of the *n*-Octane Lean Phase (L_2)

type of data	temp, K	press., atm	mole fraction of ethane	mole fraction of *n*-octane	molar vol, mL/(g mol)
K (L_1-L_2 = V)	217.66	65.4	0.138	0.0056	85.0
	214.04	62.5	0.113	0.0052	88.0
	210.95	60.2	0.100	0.0041	87.7
	206.88	57.1	0.082	0.0044	84.7
	205.98	56.6	0.077	0.0032	85.7
	205.05	56.0	0.078	0.0042	81.0
Q (S-L_1-L_2-V)	201.04	52.5	0.070	0.0063	70.4
	200.50	51.3	0.075	0.0065	69.4
	200.11	50.0	0.086	0.0089	65.4
	199.66	48.4	0.101	0.0135	63.5
	199.50	48.1	0.104	0.0141	62.7
	199.42	47.4	0.109	0.0164	62.3
	198.80	46.2	0.126	0.0216	59.9
	198.79	45.9	0.128	0.0244	60.7
	198.54	44.6	0.145	0.0338	60.3
	198.48	44.6	0.142	0.0321	59.6
	198.17	44.4	0.151	0.0362	58.3
	198.06	43.7	0.159	0.0482	59.0
LCST (L_1 = L_2-V)	214.73	61.1	0.195	0.0471	62.4
	209.68	55.4	0.197	0.0707	60.7
	207.41	53.1	0.190	0.0673	60.2
	205.36	51.0	0.185	0.0608	59.7
	204.57	50.4	0.176	0.0511	60.6
	201.93	47.4	0.187	0.0812	59.4
	200.73	46.3	0.179	0.0754	60.1
	199.42	45.0	0.183	0.0897	60.4
	198.69	44.2	0.176	0.0871	60.6
	198.52	44.1	0.181	0.0992	61.4
	198.15	43.7	0.183	0.0922	60.4
	197.80	43.3	0.185	0.0783	58.7
L_2-L_1-V	213.77	60.3	0.187	0.0367	67.7
	213.24	59.5	0.196	0.0454	65.6
	213.06	61.6	0.124	0.0067	77.7
	211.43	58.0	0.179	0.0324	65.7
	211.39	60.6	0.113	0.0067	80.3
	210.63	56.5	0.185	0.0408	63.9
	210.63	59.1	0.133	0.0109	71.3
	210.00	58.8	0.131	0.0090	69.8
	210.00	58.0	0.142	0.0139	67.0
	210.00	57.4	0.156	0.0184	64.5
	209.10	57.0	0.137	0.0145	68.6
	208.00	57.9	0.098	0.0060	77.9
	208.00	57.4	0.103	0.0080	69.3
	208.00	56.4	0.132	0.0126	67.1
	208.00	56.1	0.137	0.0141	65.7
	208.00	54.9	0.159	0.0197	62.3
	207.45	56.3	0.119	0.0102	70.0
L_2-L_1-V	206.51	56.5	0.091	0.0039	79.1
	206.28	52.6	0.170	0.0358	62.0
	206.00	56.1	0.095	0.0075	73.7
	206.00	55.4	0.103	0.0102	68.5
	206.00	55.0	0.108	0.0114	67.0
	206.00	54.2	0.130	0.0136	65.0
	206.00	53.9	0.135	0.0144	64.0
	206.00	53.7	0.140	0.0158	63.4
	206.00	52.5	0.162	0.0250	62.7
	205.45	52.5	0.154	0.0253	62.3
	205.26	52.3	0.144	0.0227	64.7
	204.00	55.0	0.073	0.0033	78.9
	204.00	54.2	0.091	0.0069	70.3
	204.00	53.6	0.098	0.0095	67.6
	204.00	52.5	0.111	0.0134	63.7
	204.00	52.1	0.129	0.0160	63.1
	204.00	51.8	0.133	0.0169	62.4
	204.00	51.2	0.143	0.0211	61.0
	204.00	50.8	0.151	0.0240	61.8
	204.00	50.3	0.162	0.0308	59.5
	203.62	50.8	0.145	0.0235	61.6
	203.03	48.8	0.172	0.0494	60.4
	202.65	48.4	0.179	0.0550	60.6
	202.18	51.9	0.085	0.0072	72.0
	202.00	53.2	0.069	0.0049	74.1
	202.00	52.5	0.075	0.0062	69.7
	202.00	52.0	0.089	0.0079	67.6
	202.00	51.6	0.093	0.0088	66.3
	202.00	51.1	0.100	0.0116	64.8
	202.00	50.1	0.113	0.0157	62.2
	202.00	49.8	0.127	0.0179	61.6
	202.00	49.6	0.131	0.0194	61.1
	202.00	48.8	0.145	0.0256	59.6
	202.00	48.4	0.155	0.0288	60.7
	202.00	47.9	0.164	0.0387	58.2
	201.84	49.3	0.125	0.0195	62.6
	200.79	46.5	0.171	0.0518	59.5
	200.77	46.7	0.165	0.0471	60.1
	200.00	48.7	0.103	0.0136	63.0
	200.00	47.7	0.116	0.0184	61.1
	200.00	47.6	0.126	0.0187	60.4
	200.00	47.2	0.134	0.0214	59.8
	200.00	46.4	0.148	0.0294	58.8
	200.00	46.0	0.157	0.0364	59.8
	199.86	47.2	0.127	0.0223	61.1
	199.71	45.5	0.161	0.0460	59.3

rich L_1 phase compositions were determined, the cell was only 40–75% full of L_1 since a sizable amount of L_2 and V were needed to accurately judge the critical point. However, the L_2 = V phase compositions were determined accurately with 90% or more of the cell containing L_2 = V. The L_2 = V data were then used to accurately calculate L_1 phase compositions.

Lower critical solution temperature points (LCST) were obtained by decreasing temperature until significant amounts of L_1 and L_2 became critically identical. For these points, the volume of L_1 = L_2 was usually 85% or more of the cell. Many L_1–L_2–V points were obtained during the experimental approach to the Q, K, and LCST points. A L_1–L_2–V point was taken when one of the liquids filled 80% of the cell volume and the other liquid filled less than 5%.

Temperatures were measured with a platinum resistance thermometer which was accurate to at least ±0.03 K of the 1968 IPTS scale. Pressure measurements were taken with a Heise Bourdon tube gage which was accurate to at least ±0.07 atm. The gage was occasionally compared to a dead-weight piston gage. Liquid-phase volumes could be read to ±0.02 mL. The weight of *n*-octane was determined on an analytical balance to ±0.0001 g. The volume of methane and ethane gas displaced by mercury was known to a probable error of ±0.006 mL (±0.000 02 g mol).

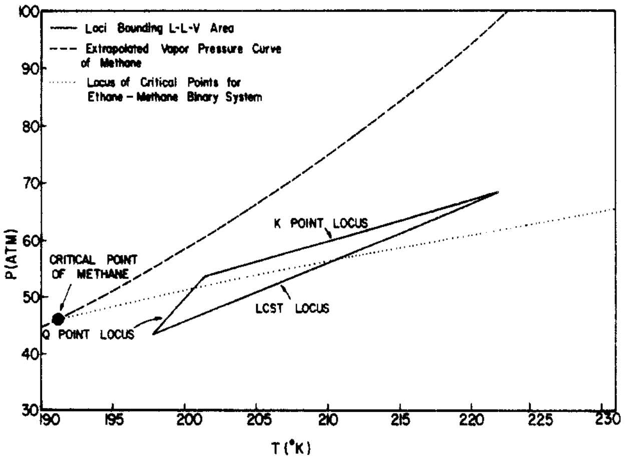

Figure 1. *P*–*T* Immiscibility area for methane–ethane–*n*-octane system.

Table II. Raw Data of the *n*-Octane Rich Phase (L_1)

type of data	temp, K	press., atm	mole fraction of ethane	mole fraction of *n*-octane	molar vol, mL/(g mol)
K (L_1-L_2 = V)	219.25	66.4	0.240	0.093	63.8
	214.26	62.6	0.222	0.141	66.1
	213.64	62.1	0.234	0.148	66.1
	212.63	61.4	0.220	0.157	67.2
	208.72	58.5	0.188	0.209	74.1
	203.84	55.1	0.145	0.277	80.8
	202.02	53.8	0.136	0.304	83.6
	201.91	53.7	0.130	0.300	82.2
Q (S-L_1-L_2-V)	200.85	52.3	0.125	0.274	75.4
	200.65	51.6	0.132	0.273	75.6
	200.26	50.5	0.133	0.252	73.1
	200.21	50.2	0.145	0.245	72.0
	199.33	47.4	0.155	0.209	69.9
	198.51	44.9	0.182	0.157	66.0
	198.40	44.8	0.175	0.155	64.9
	198.35	44.8	0.177	0.154	64.5
	198.08	43.7	0.177	0.120	62.6
L_1-L_2-V	218.21	64.8	0.231	0.087	64.9
	213.79	61.8	0.210	0.142	68.1
	210.00	59.4	0.199	0.188	70.1
	210.00	58.7	0.196	0.164	65.6
	210.00	57.0	0.202	0.131	64.2
	208.00	57.4	0.181	0.194	69.5
	208.00	56.7	0.184	0.176	66.6
	208.00	55.8	0.194	0.159	65.9
	208.00	54.3	0.196	0.124	64.4
	208.00	53.8	0.204	0.092	62.1
	206.10	56.4	0.158	0.230	75.2
	206.00	55.2	0.180	0.197	69.2
	206.00	54.1	0.185	0.176	67.3
	206.00	53.2	0.194	0.155	65.7
	206.00	52.0	0.203	0.116	62.4
L_1-L_2-V	205.25	51.1	0.200	0.111	63.0
	205.25	50.8	0.199	0.099	62.5
	204.00	52.8	0.171	0.199	68.9
	204.00	51.6	0.182	0.171	66.9
	204.00	50.8	0.189	0.148	64.2
	204.00	49.7	0.198	0.102	60.1
	203.47	48.9	0.194	0.096	62.1
	203.00	52.0	0.158	0.219	71.9
	202.00	52.9	0.138	0.255	73.5
	202.00	52.7	0.139	0.250	72.8
	202.00	50.4	0.165	0.199	68.4
	202.00	49.1	0.179	0.167	66.1
	202.00	48.5	0.187	0.144	64.3
	202.00	47.4	0.189	0.083	59.4
	200.72	46.2	0.186	0.091	61.0
	200.00	47.9	0.161	0.192	66.8
	200.00	46.7	0.178	0.161	65.4
	200.00	46.2	0.184	0.139	63.4
	198.52	44.3	0.177	0.121	62.7

Results

Raw L–L–V experimental data for the ternary system methane–ethane–*n*-octane are presented in Tables I and II. Table I presents composition and molar-volume data of the octane lean-liquid phase (L_2) for type-K (L_1–L_2 = V), type-Q (S–L_1–L_2 = V), and LCST (L_1 = L_2–V) points which surround the area of immiscibility. Table I also reports L_2 information for 63 points within the L–L–V region. The standard deviations of the K, Q, and LCST data points from smooth lines that define the L–L–V region are 1.5% for the *n*-octane mole fraction in L_1, 6.0% for the *n*-octane mole fraction in L_2, 1.7% for the mole fraction of ethane, 1.1% for the molar volume, and 0.3% for the pressure. This is consistent with error analyses in similar work by the authors whose liquid-phase solute composition was reliable to ±2%.

Figure 1 shows the immiscibility area bounded by loci of type K and type Q and LCST points in pressure–temperature space at 197.8 K and 43.3 atm to ~222 K and 69 atm. In the *P*–*T* space are three unique points of zero degrees of freedom. They are the point of intersection of the Q locus with the LCST locus (S–L_1 = L_2–V), the point of intersection of the Q locus and the K locus (S–L_1–L_2 = V), and the intersection of the K locus with the LCST locus (L_1 = L_2 = V), known as the tricritical point. The location of the tricritical point is an estimate.

Figure 1 also shows the extrapolated vapor-pressure curve for methane (*15*) and the locus of type-K points for the binary methane-ethane system (*16*, *7*). The region of immiscibility falls below the extrapolated vapor-pressure curve and on top of the binary critical locus. The *n*-octane lean phase behaves similarly to the liquid phase in an ethane–methane binary system with the locus of type-K points for the ternary system falling from 2 to 6 atm above the binary critical locus.

Literature Cited

(1) Lin, Y-N.; Chen, R. J. J.; Chappelear, P. J. Kobayashi, R. *J. Chem. Eng. Data* **1977**, *22*, 402.
(2) Lin, Y-N.; Hwang, S. C.; Kobayashi, R. *J. Chem. Eng. Data* **1978**, *23*, 231.
(3) Tiffin, D. L.; Luks, K. D.; Kohn, J. P. *Adv. Cryog. Eng.* **1978**, *23*, 538.
(4) Kohn, J. P.; Bradish, W. F. *J. Chem. Eng. Data* **1964**, *9*, 5.
(5) Carfagno, J. A.; McCaffrey, D. S.; Kohn, J. P. *J. Chem. Eng. Data* **1967**, *12*, 289.
(6) Kohn, J. P.; Kim, Y. J.; Pan, Y. C. *J. Chem. Eng. Data* **1966**, *11*, 333.
(7) Wagner, J. R.; McCaffrey, D. S., Jr.; Kohn, J. P. *J. Chem.* Eng. Data **1968**, *13*, 22.
(8) Rowlinson, J. S. "Liquids and Liquid Mixtures", 2nd ed.; Butterworth: London, 1968, p 214.
(9) Green, K. A.; Tiffin, D. L.; Luks, K. D.; Kohn, J. P. *Hydrocarbon Processing* 1979, *58* (5), 251.
(10) Orozco, C. E., Tiffin, D. L., Luks, K. D., and Kohn, J. P., *Hydrocarbon Process*. **1977**, *56*, 325.
(11) Goodwin, R. D.; Roder, H. M.; Straty, G. C. *NBS Tech. Note (U.S.)* **1976**, *No. 684*.
(12) Kohn, J. P. *AIChE J.* **1961**, *7*, 514.
(13) Tiffin, D. L.; Kohn, J. P.; Luks, K. D. *J. Chem. Eng. Data* **1979**, *24*, 306.
(14) Wichterle, I.; Kobayashi, R. *J. Chem. Eng. Data* **1972**, *17*, 9.
(15) Clark, A. M.; Din, F. *Trans. Faraday Soc.* **1953**, *49*, 202.
(16) Hicks, C. P.; Young, C. L. *Chem. Rev.* **1975**, *75*, 119.

Received for review June 9, 1980. Accepted December 22, 1980.